

Appendix

A Determination of timestep size

In this section, the value of Δt for UPL, SFMc, and SFMe is estimated in order to avoid numerical instability in such simulations. Multiple simulations are performed by varying Δt from 0.5 s to 10^{-5} s (Figures A-1-A-3). Note that ten different offsets (deviation from the original position) are simulated for each Δt since the behavior strongly depends on the magnitude of the offset. If we look at the figures, we will observe that in the cases of UPL, SFMc, and SFMe, the trajectories converge at 0.01s. Zoomed figures are also plotted in figures. The author has also set the value of time iteration as 0.01s in the cases of CFMc and CFMe. Hence, $\Delta t = 0.01s$ is set for all the models in this study.

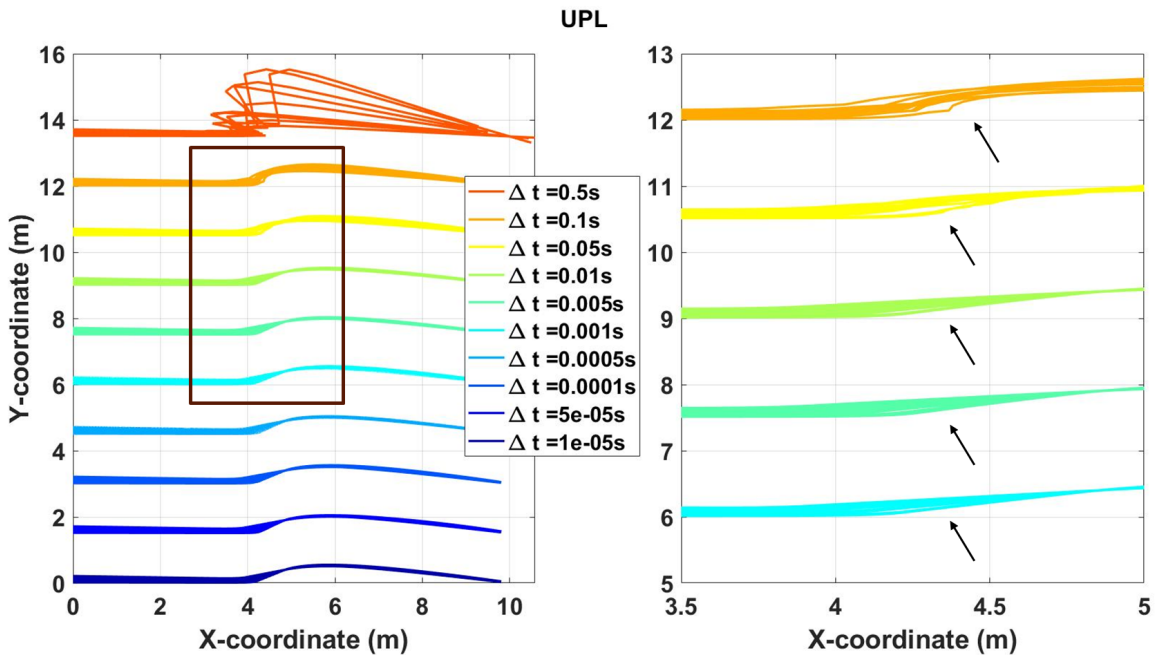


Figure A-1: Trajectories of SOSP case with different values of Δt simulated using UPL model (right). A magnified view of trajectories within the black rectangular box is given on the left side, highlighting the convergence of trajectories after $\Delta t = 0.01 s$

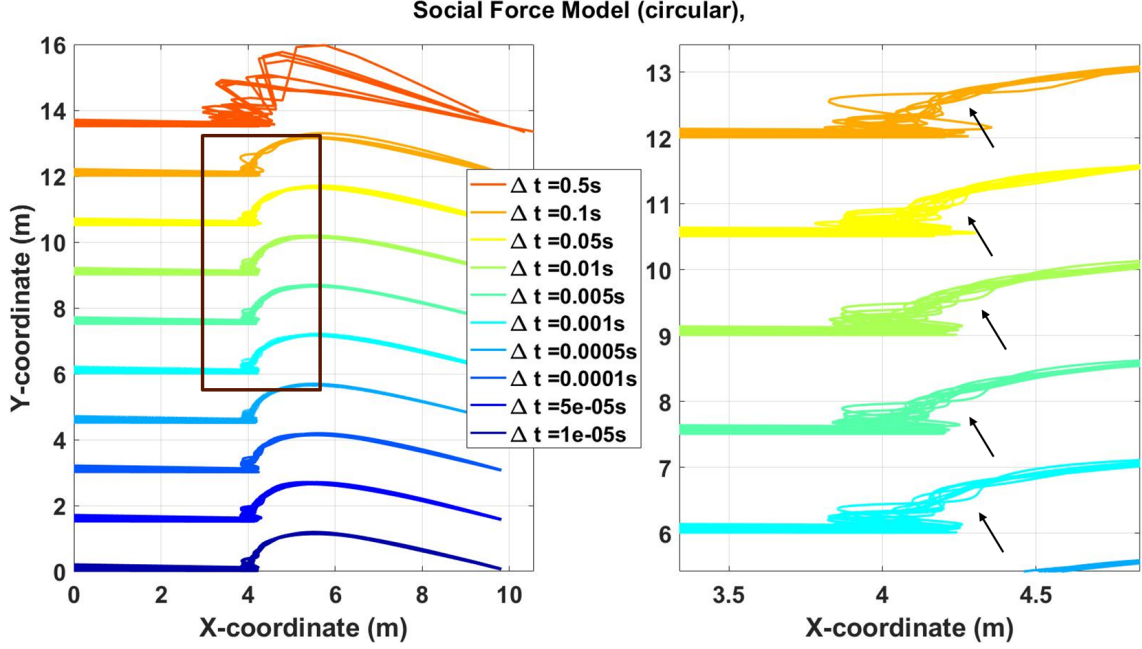


Figure A-2: Trajectories of SOSP case with different values of Δt simulated using SFMc model (right). A magnified view of trajectories within the black rectangular box is given on the left side, highlighting the convergence of trajectories after $\Delta t = 0.01$ s

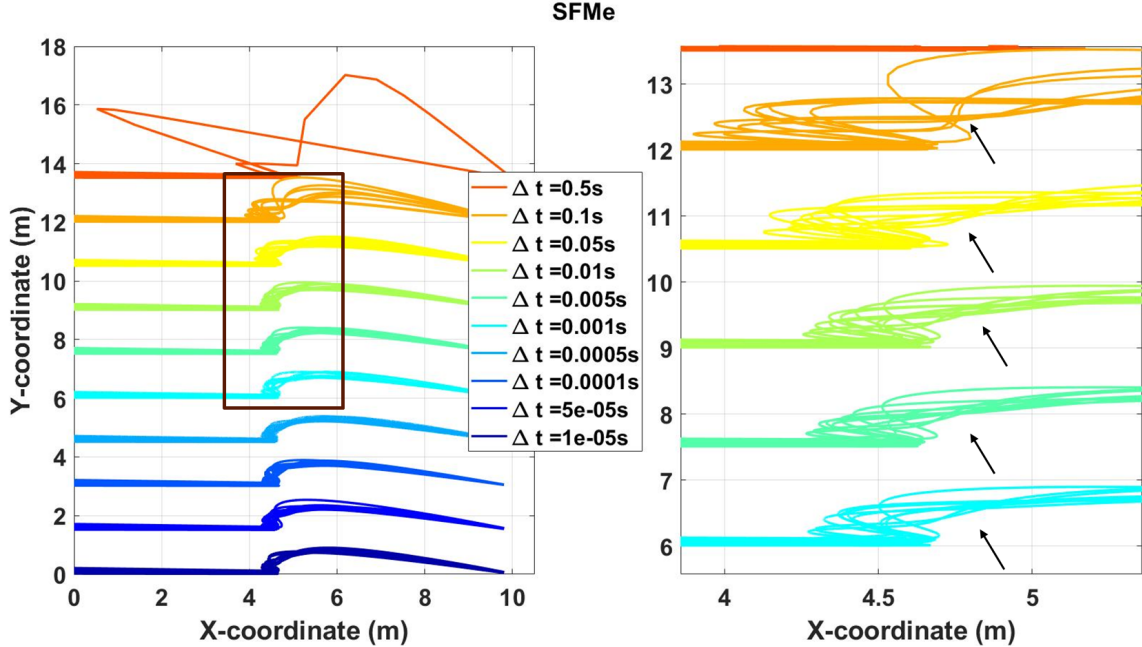


Figure A-3: Trajectories of SOSP case with different values of Δt simulated using SFMe model (right). A magnified view of trajectories within the black rectangular box is given on the left side, highlighting the convergence of trajectories after $\Delta t = 0.01$ s

B Simulation Results for MOSP

In Figure B-4, normalized speed averaged over all the trajectories are plotted with respect to x coordinates of the pedestrian position for all four cases. During the experiment, pedestrians tend to maintain their desired speed, however, minor irregularities and speed deviations can be observed due to frequent changes in direction caused by the presence of multiple obstacles. In contrast, all the models exhibit significant deviations from the desired speed, especially in high-density cases. Notably, the SFMc model displays a near-perfect speed profile, which is attributed to its weak interaction force, allowing pedestrians to pass through the obstacle maze by overlapping with obstacles

without altering their path, also shown by a trajectory in Figure B-5(a). Additionally, the SFMe model shows an average speed approaching 0 m/s in Cases C and D due to excessively large interaction forces that immobilize pedestrians even before they enter the obstacle maze, also observed by the pedestrian trajectory in Figure B-5(b).

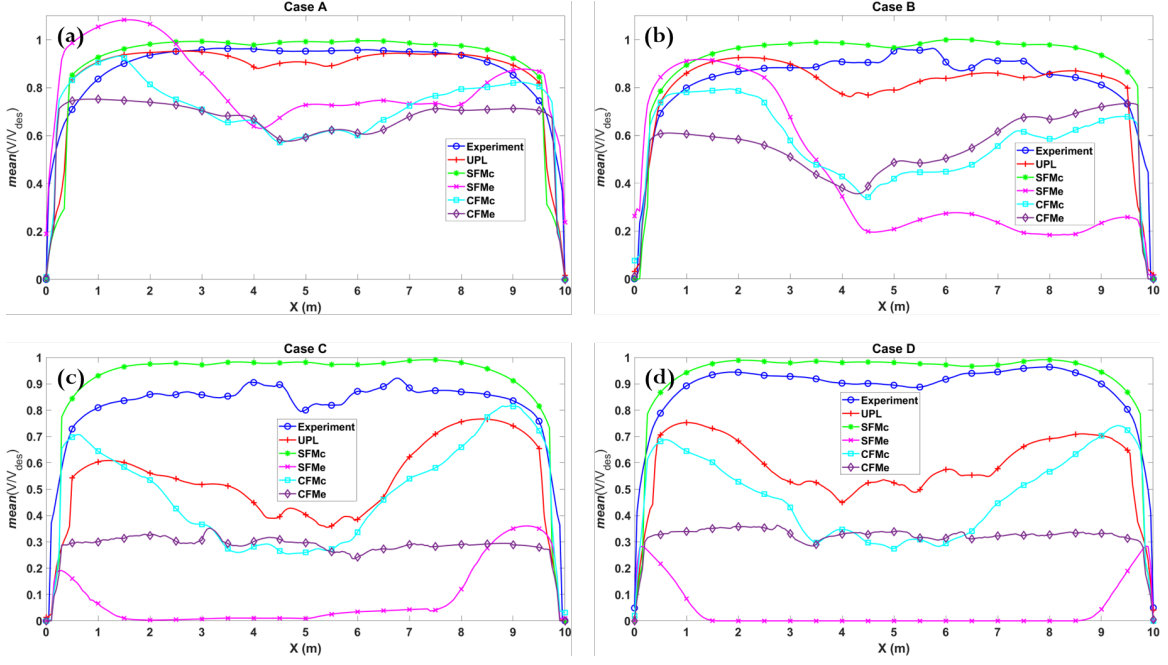


Figure B-4: Normalized speed averaged over all the trajectories are plotted with respect to x coordinates of the pedestrian position for all four cases.

Social Force Model unrealistic behaviour

During simulations, both the SFMc and SFMe models exhibited unrealistic results, particularly in MOSP scenarios. In Figure B-5(a), one of the trajectories of the SFMc model for MOSP Case D is shown. This trajectory indicates that the pedestrian passes through the maze of obstacles without altering its path to avoid them, resulting in overlaps. Consequently, as illustrated in the figure, the SFMc model only registers successful cases when the obstacle configuration is favorable, rather than attempting to avoid obstacles. Similarly, Figure B-5(b), shows one of the trajectories for the SFMe model for MOSP Case C. This trajectory shows the pedestrian becoming immobilized without even entering the measurement zone. For the SFMe model, the interaction forces' values become excessively large due to the presence of multiple obstacles, rendering the pedestrian stationary, which is clearly unrealistic.

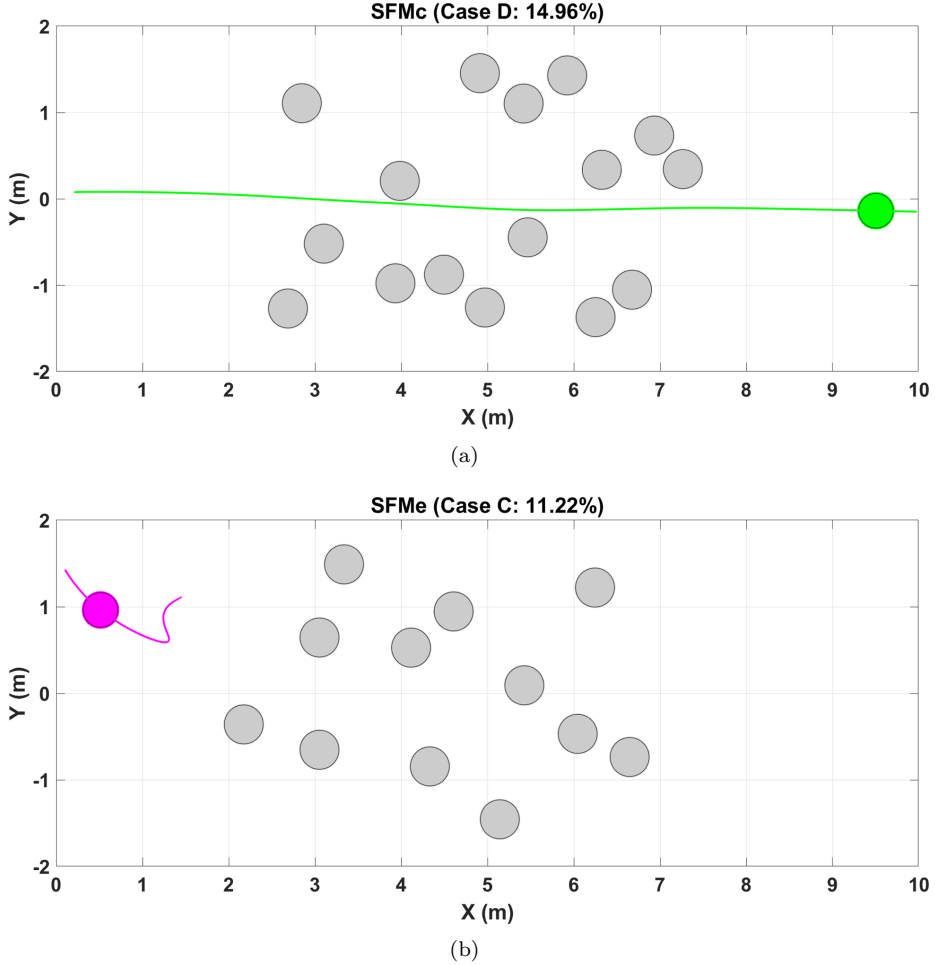


Figure B-5: Trajectories graphs for a) SFMc (MOSP Case D) and b) SFMe (MOSP Case C), showing unrealistic simulation results.

C Parameter selection for Social Force Models

The values of parameters for SFMc and SFMe were taken from the study by Johansson et. al. [1]. The authors provided two sets of calibrated values for the constants A and B. One set assumes no angular dependency in the social force ($\lambda = 1$), while the other set includes angular dependency ($\lambda \neq 1$). Ideally, angular dependency should be considered in any social force model to accurately represent pedestrian behavior. However, our simulations of multiple obstacle scenarios using SFMc and SFMe with $\lambda \neq 1$ revealed significant issues. Detailed pie charts illustrating findings for SFMc and SFMe are shown in Figure C-6. We observe a large share of failed simulations with a low incidence of failures due to pedestrians getting stuck. Instead, most failures occurred because trajectories resulted in $\geq 50\%$ overlap with obstacles. This suggests that the magnitude of the forces experienced by pedestrians was insufficient to avoid obstacles, leading to excessive overlap. This outcome indicates a fundamental problem in social force failing to help avoid the obstacles when angular dependency is considered. Consequently, for our study, we opted to use the calibrated values of constants A and B for the case where $\lambda = 1$.

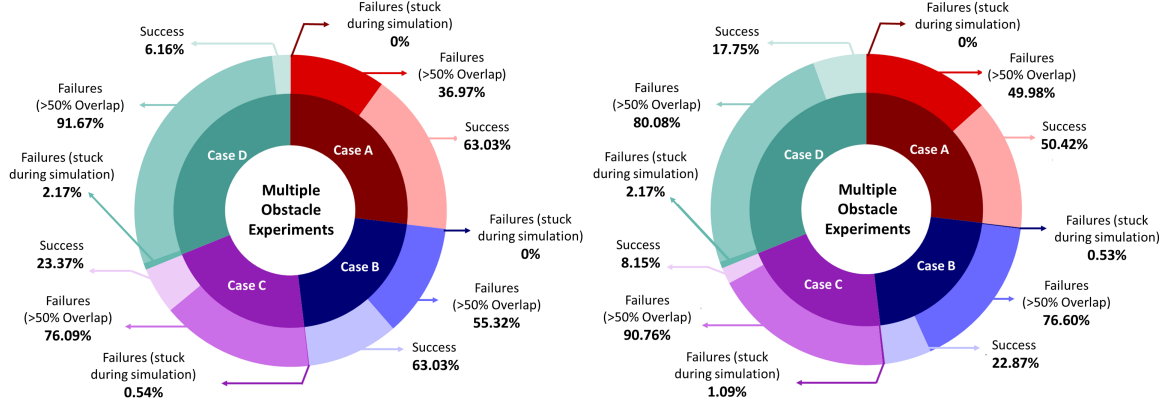


Figure C-6: Detailed pie charts for (a) SFMc and (b) SFMe when angular dependency is considered during simulation. Multiple obstacle experiments are reproduced using SFMc and SFMe for four different cases: Case A (3.74% of area covered by obstacles), Case B (6.54% of area), Case C (11.22% of area), and Case D (14.96% of area). The figures show a large share of failed simulations in all four cases, with most failures due to more than 50% overlap with obstacles, while only a few (or none in some cases) are due to simulations getting stuck. This indicates that pedestrians are unable to effectively avoid the obstacles, resulting in significant overlap when utilizing the social force model with angular dependency.

D Single Pedestrian Single Obstacle

All the trajectories and velocities generated by the reproducing experiment are shown in Figure D-7. In the case of UPL, neither oscillations nor overlaps are present in any of the trajectories. However, the sudden dip in speeds while crossing the obstacle can be observed, especially in the cases of low offset (Figure D-7(a)). For SFMc, we can see the sudden change in direction and multiple oscillations in each and every trajectory (Figure D-7(b)). Similarly, in the case of SFMe, sudden changes in directions and oscillations are present. However, in this case, pedestrians reach closer to the obstacle, and the number of times pedestrians oscillate is lower, (Figure D-7(c)). No oscillations are predicted in the case of centrifugal force models, but overlaps are present, especially for the low offsets in the case of CFMc (Figure D-7(d)) and sudden change in directions in the case of CFMe, (Figure D-7(e)).

E Model evaluation for different parameters

While it is true that parameter tuning (e.g., adjusting k and τ_0 in the case of UPL) can influence model behavior, our additional analysis (see Figure E-8) demonstrates that even significant variations (up to tenfold changes) in these parameters do not substantially improve the model's performance in the tested scenarios. This supports the article's focus on addressing deeper structural issues in the models, rather than parameter sensitivity alone.

References

- [1] Anders Johansson, Dirk Helbing, and Pradyumn K Shukla. Specification of the social force pedestrian model by evolutionary adjustment to video tracking data. *Advances in complex systems*, 10(sup02):271–288, 2007.

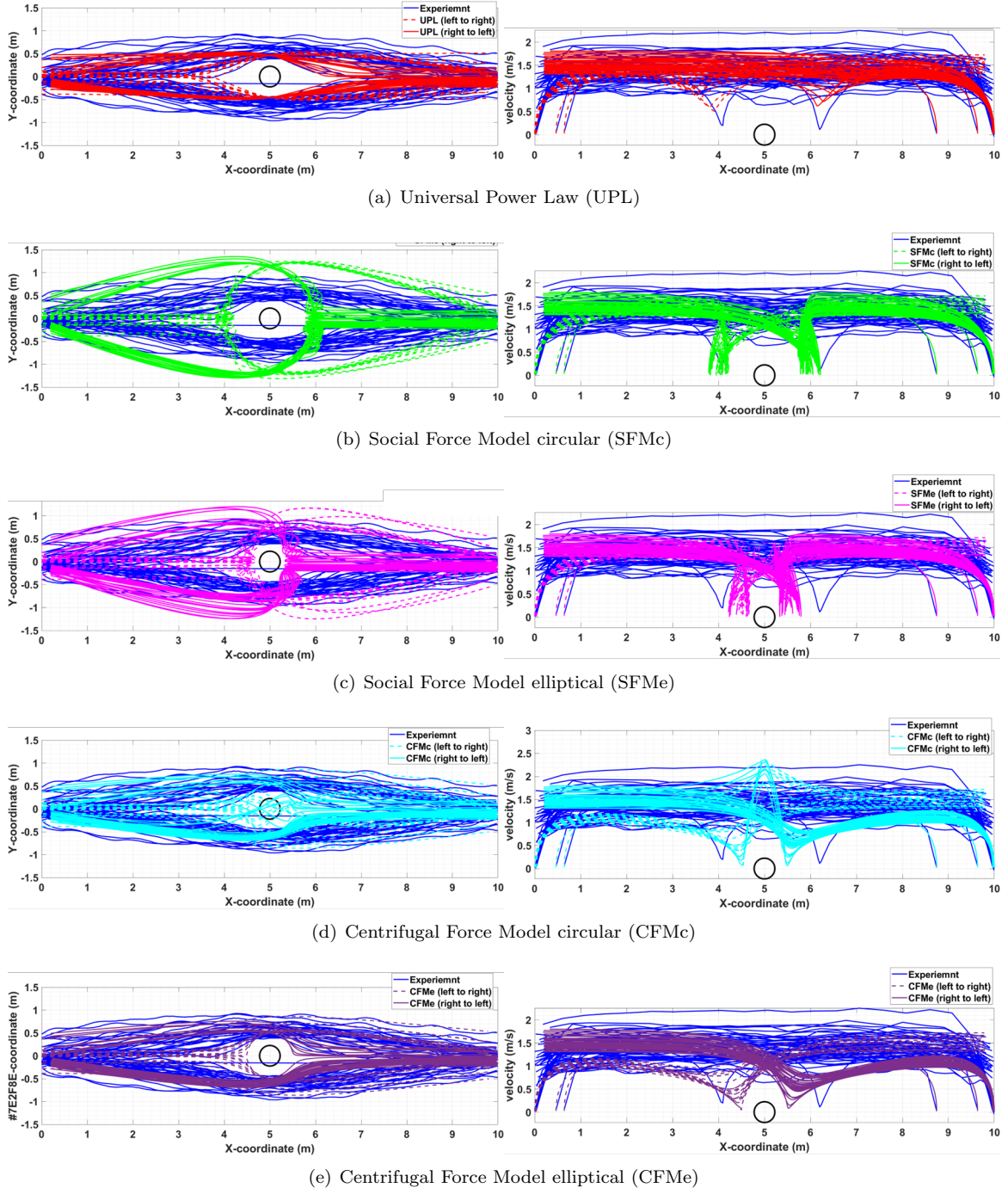


Figure D-7: Trajectories and velocity graphs are generated using all the force-based models and are compared with the experiment.

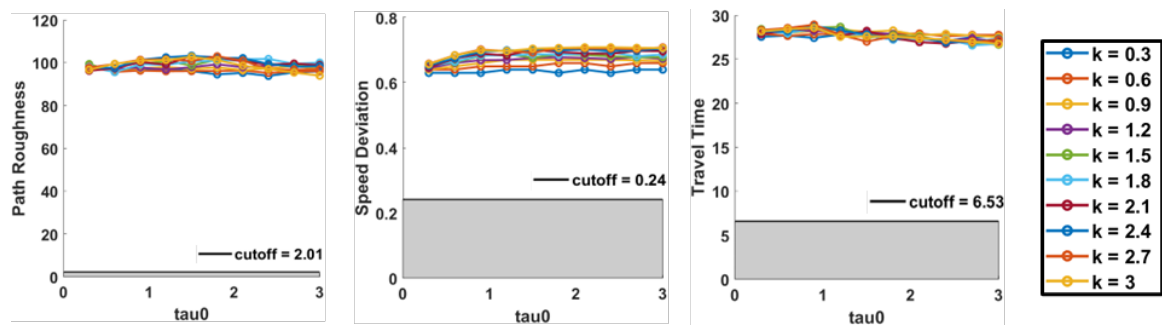


Figure E-8: The values of evaluating metrics by varying parameters k and τ_0 in the case of UPL for the MOSP (Case D) scenario.